

# Design of a Pulse Transformer for X-band Klystron

Yongfang Liu, Yonghua Wu, Xiaoxuan Zhou, and Jin Tong\*

Shanghai Advanced Research Institute  
Chinese Academy of Sciences, Shanghai, 201204, China  
liuyongfang@sari.ac.cn, wuyh@sari.ac.cn, zhouxx@sari.ac.cn, tongj@sari.ac.cn  
\*Corresponding author

**Abstract** – Future linear accelerators require klystrons with higher radio frequency (RF) to drive higher gradient accelerating structure. An x-band accelerator structure was used to accelerate electrons at the Shanghai Soft X-ray Free Electron Laser Facility (SXFEL) in Shanghai Advanced Research Institute, Chinese Academy of Sciences (SARI-CAS). A pulse transformer is a crucial device in an RF system. This study presents a high-voltage pulse transformer used for a 50 MW x-band pulsed klystron in SXFEL. Typical specifications of the pulse transformer are peak pulse voltage 420 kV, peak pulse current 300 A, 50 Hz repetition rate and 1.5  $\mu$ s flat-top pulse width. Design and optimization of pulse transformer are achieved by using equivalent circuit analytic methods and computational aided simulation. The relevant experiments show that this pulse transformer can meet the requirements of 50MW x-band klystron.

**Index Terms** – flat-top, klystron, pulse modulator, pulse transformer, rise time.

## I. INTRODUCTION

X-ray free electron lasers (XFEL) are regarded as a new generation of advanced light sources. Shanghai Soft X-ray Free Electron Laser Facility, which is the first coherent x-ray light source in China, started user operation in 2023 and opened to scientists both from home and abroad [1]. The RF system of SXFEL's main accelerator adopts s-band, c-band and x-band technology, including five s-band RF units, fifteen c-band RF units and two x-band RF units. The RF unit is mainly composed of a klystron amplifier, a low-level RF (LLRF) system, a pulse modulator and a pulse transformer [2]. An X-band RF unit is used to achieve higher gradients (80 MV/m) and more compact footprints for SXFEL's main accelerator, which is driven by a pulsed 50MW x-band klystron. The pulse transformer which provides cathode voltage for the klystron connects the pulse modulator and klystron. Generally, a pulse transformer realizes voltage converting, dc isolation, matching impedances, polarity inversion and power delivery from the primary side to the secondary side. Figure 1 shows a typical schematic of a

pulse transformer circuit. The x-band RF unit requires a high-power pulse transformer to drive the 50 MW x-band klystron [3–7]. A pulse transformer is a crucial device in an RF unit. The specifications of the high-voltage pulse transformer are listed in Table 1. Table 2 shows the performance of the x-band pulse transformers in other research institutions [8].

In this study, a high-power pulse transformer is developed. The design needs to guarantee the transformer with a fast leading and falling time, a minimum of overshoot and flat-top ringing. The optimized design method of electromagnetic devices like this pulse transformer can depend on an equivalent circuit model and computational aided simulation. The pulse transformer's design procedure, with all the basic stages, is given. Spice circuit simulation software (LTspice) and finite element analysis software (Comsol) are used to verify the design. Test data and waveforms are provided. The results indicate that the high-power pulse transformer meets requirements. The pulse transformer has been continuously operated for over two years without any failures.

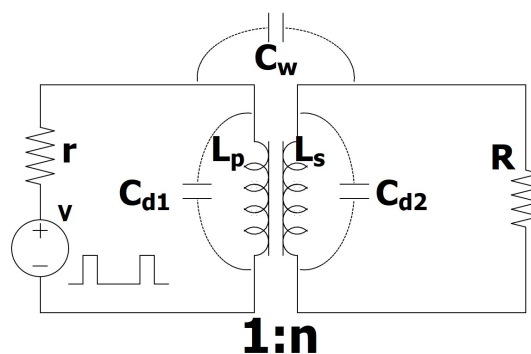


Fig. 1. A typical pulse transformer circuit.  $V$  is the source of the ideal pulse,  $r$  is resistance of pulse source,  $C_{d1}$  and  $C_{d2}$  are winding line distribution capacity,  $C_w$  is stray capacitance between primary and secondary windings,  $L_p$  and  $L_s$  are primary and secondary inductance,  $R$  is load.

Table 1: Specifications of the pulse transformer

Items	Value
Peak output power	126 MW
Primary nominal voltage	22 kV
Primary current	5700 A
Secondary voltage	420 kV
Secondary current	300 A
Pulse flat-top	1.5 $\mu$ s
Pulse overshoot	$\leq$ 1%
Pulse repetition rate	50 Hz
FWHM	3.5 $\mu$
Insulating material breakdown field	10 kV/mm
Relative permittivity of insulating oil	3
Relative permeability of core material	3500

Table 2: Performance of the x-band pulse transformers in other research institution

Items	KEK	SLAC	CECT
Pulse voltage (kV)	500	464	446
Pulse current (A)	301	190	187
Repetition rate (Hz)	200	120	10
Flat-top ( $\mu$ s)	0.5	1.5	1.5

## II. ELECTRICAL AND MECHANICAL DESIGN

The role and function of pulse transformer is to step-up pulse voltage from 22 kV to 420 kV with small flat-top drop, small overshoot and low oscillations. The transformer is of rectangular type core and is constructed with cool-rolled silicon steel sheets. In this section, electrical design and relevant geometrical parameters of the pulse transformer are provided and discussed.

### A. Electrical circuit

A high-voltage pulse transformer is designed for x-band modulator and klystron. In this design, a filament heating power supply and a pump power supply are required for the x-band klystron cathode, so the pulse transformer adopts a scheme of four secondary windings. Figure 2 shows the practical schematic of the pulse transformer in the linear modulator. In pulse transformer, magnetic flux swings in one direction only, not fully utilizing the core. To avoid flux saturation, core reset circuits named bias power supply (PS)PS are used. The primary winding receives the output pulse waveform of pulse modulator. The filament heating power supply and

pump power supply use two secondary windings separately. The secondary winding generates an induced high-voltage pulsed waveform.

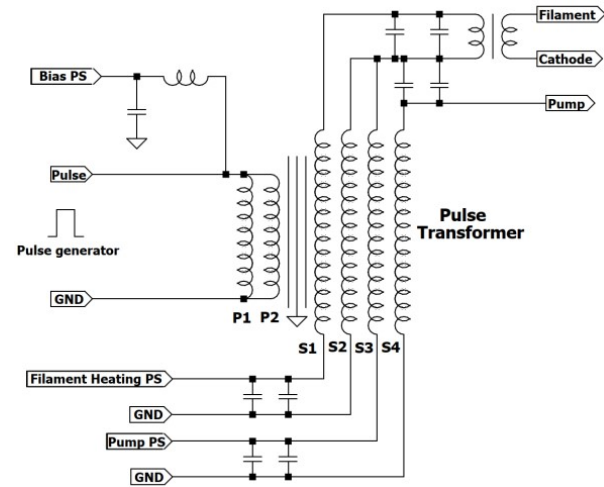


Fig. 2. Detailed circuit of pulse transformer application.

### B. Ratio of pulse transformer

In this high-voltage pulse transformer, the secondary peak pulse voltage is 420 kV and the maximum primary peak pulse voltage is 25 kV, which is equal to half of the charging power supply. The minimum ratio of pulse transformer can be calculated as follows:

$$n = \frac{V_S}{V_p}, \quad (1)$$

where  $n$  is transformer ratio,  $V_S$  is the secondary peak pulse voltage, and  $V_p$  is the primary peak pulse voltage. The ratio of the pulse transformer is selected as 1:19 in consideration of suitable margins.

### C. Coil Turns and core cross-sectional area

The primary winding turns, the secondary winding turns, and the minimum cross-sectional area of the core are determined by the following equations:

$$N_p = \frac{V_p T_p}{A_{core} \Delta B} \quad (2)$$

$$N_s = n N_p \quad (3)$$

$$A_{core} = \frac{1}{N_p \Delta B} (V_p T_p) \quad (4)$$

where  $N_p$  and  $N_s$  are the primary and secondary winding turns,  $T_p$  is the pulse width at full width at half maximum (FWHM),  $\Delta B$  is increment of magnetic induction intensity,  $A_{core}$  is the minimum cross-sectional area of the core to avoid saturation. The primary coil is designed as two 5-turn windings in parallel, and the secondary coil is designed as four 95-turn windings in parallel.

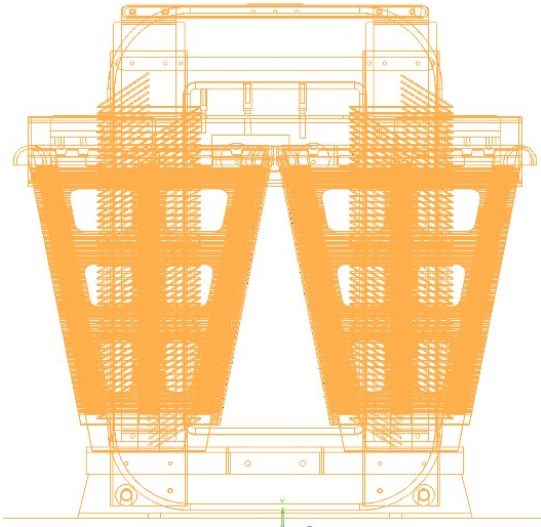


Fig. 3. The mechanical design of the pulse transformer.

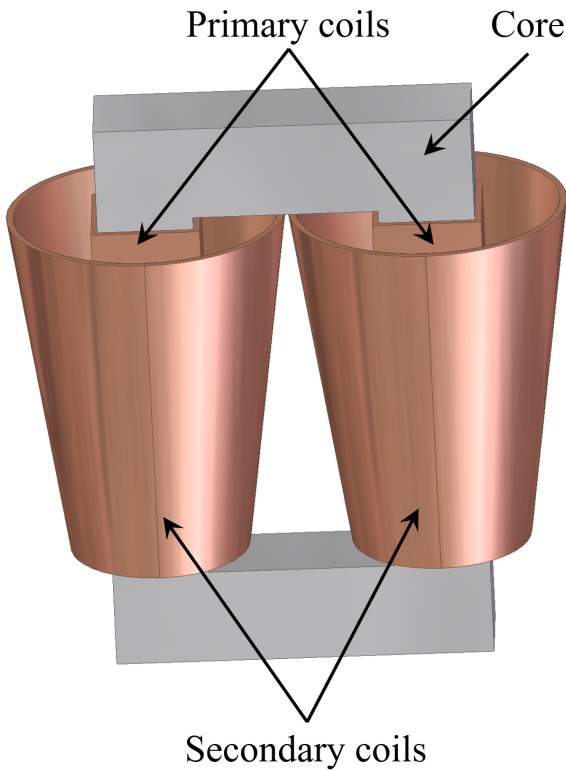


Fig. 4. 3D view of the pulse transformer structure.

The cross-sectional area of the core is designed as 112 cm<sup>2</sup>. The geometric shape of the core is almost rectangular, except for the corners which are rounded. High-quality cool-rolled silicon steel sheets are chosen as the core's material.

#### D. Mechanical design

In order to ensure sufficient insulation distance, a wedge with an inverted trapezoidal cross section is designed as the secondary winding. The core is fixed to a ground plane covered with a special glass fiber layer. The secondary winding is supported by a fiberglass braced structure which surrounds the core. Creepage and clearance distances are the main considerations in the design. The transformer, together with the protective circuit and measuring circuit is placed in a metallic tank holding electric insulating oil which serves both as insulator and coolant. The primary winding is separated from secondary by a gap of 46 mm in case of electric spark due to insufficient insulation distance. In the transformer operation, heat is generated due to losses in windings caused by Joule heating and the core caused by hysteresis, eddy and anomalous effects. An efficient cooling system is necessary in order to minimize the risk of temperature rise. Figure 3 shows the mechanical design of the pulse transformer and Fig. 4 shows the 3D view of the pulse transformer structure.

### III. MODEL ANALYSIS

#### A. Equivalent circuit of pulse transformer

In transformers, the time variation of the magnetic flux passing through the secondary coil depends on the current change of the primary coil [9–11]. The primary input of a pulse transformer is a pulse waveform generated by a pulse modulator. In fact, due to a finite frequency band of pulse transformers, output waveforms in the secondary side have a finite rise time, an overshoot, a flat-top droop and a backswing at fall time [12]. The principle of the pulse transformer is the same as an ordinary transformer. However, pulse transformer handles not a simple sine wave but a pulse waveform with complex spectrum. In the case of an ideal rectangular pulse, there is no rise time, no overshoot, a completely flat top and also no backswing.

The pulse transformer's equivalent circuit model including a pulse generator and a load is presented in Fig. 5.

#### B. Rise time

Generally, in the equivalent circuit of Fig. 4, it is possible to ignore  $R_e$ ,  $C_d$  and  $C_L$  when analyzing the leading edge [13–15]. Then, the equivalent circuit for leading edge analysis can be given as shown in Fig. 6. We can obtain the leading edge by solving differential equation of second order circuit, the leading edge is calculated as follows:

$$T_r = 2\pi y(\sigma) \sqrt{L_e C_d} \quad (5)$$

where  $L_e$  denotes the leakage inductance,  $C_d$  denotes the distributed capacitance,  $R_L$  denotes the load

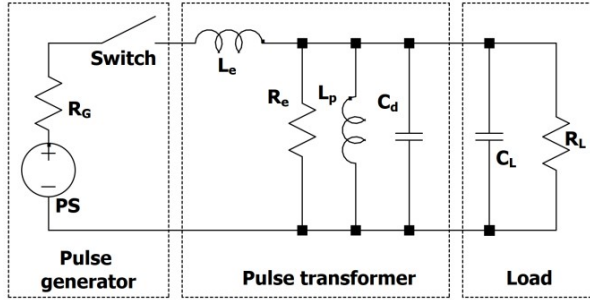


Fig. 5. Equivalent circuit model of the pulse transformer.  $R_G$  means the impedance of power supply,  $L_e$  indicates the leakage inductance,  $R_e$  means equivalent impedance of eddy current loss,  $L_p$  is the primary coil inductance,  $C_d$  is stray capacitance between coils and grand,  $C_L$  means the load stray capacitance, and  $R_L$  means impedance at primary side.

impedance.  $\sigma = \frac{Z_T}{2R_L}$ ,  $Z_T = \sqrt{\frac{L_e}{C_d}}$  and  $y(\sigma)$  is a monotonically increasing function of the damping coefficient  $\sigma$ . It is obvious that leading edge depends on the pulse transformer distribution capacitance and leakage inductance. It is evident that small overshoot leads to short pulse rise time.

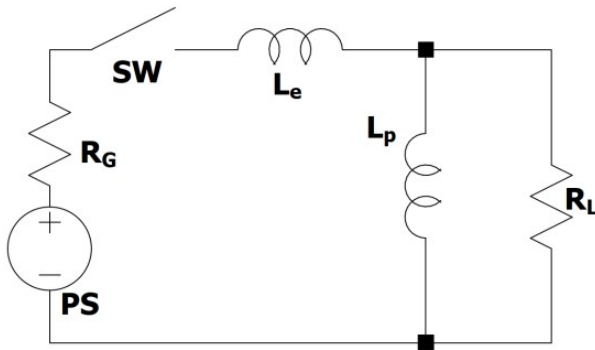


Fig. 6. Equivalent circuit for leading edge analysis.

In the pulse transformer design, leakage inductance is of considerable importance due to high insulation distance between the primary and secondary winding resulting in flux leakage [16]. For simulation of pulse transformer to evaluate leakage inductance, Comsol Multiphysics, which is a simulation tool for solving electromagnetic problems, is used. Magnetostatic simulation is used for the evaluation of leakage inductance of pulse transformer [17]. The model is specified in Comsol Multiphysics, together with material parameters, boundary conditions and other needed input values such as excitation current and frequency. Figure 7 shows the magnetic flux density of the designed pulse transformer. The leak-

age inductance simulation result is 1.78  $\mu\text{H}$ . From leading edge calculation formula, it can be seen that the larger leakage inductance, the slower leading edge, and the smaller the distributed capacitance, leading to faster leading edge and smaller overcharge.

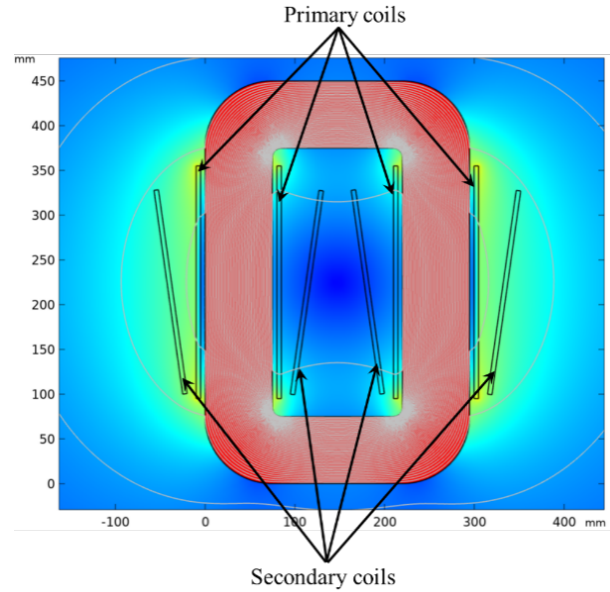


Fig. 7. Magnetic flux density of the designed pulse transformer.

### C. Flat-top droop

In the flattop of the pulse waveform, pulse transformer behaves as a low-frequency equipment, due to the invariant voltage over time [18–19]. Thus, elements that are involved in the high-frequency component for  $L_e$ ,  $C_d$ ,  $C_L$  and  $R_e$  can be ignored. Then, the equivalent circuit of Fig. 4 may be rewritten as in Fig. 8. According to Kirchhoff's voltage law, the voltage on the load  $R_L$  can be expressed as follows:

$$U_L = \alpha E e^{-\frac{t}{T_d}} \quad (6)$$

$$\alpha = \frac{R_L}{R_L + R_{PFN}} \quad (7)$$

$$T_d = \frac{L_p(R_L + R_{PFN})}{R_L R_{PFN}} \quad (8)$$

where  $E$  is the voltage of the pulse,  $\alpha$  is the pulse transformer primary to secondary transfer factor.  $T_d$  is the time constant of the pulse transformer. The flat-top droop is denoted by  $D$ , which is defined as follows:

$$D = 1 - e^{-\frac{t}{T_d}} \quad (9)$$

From Equations (6) to (9), the primary inductance of the pulse transformer is related to the top drop as follows:

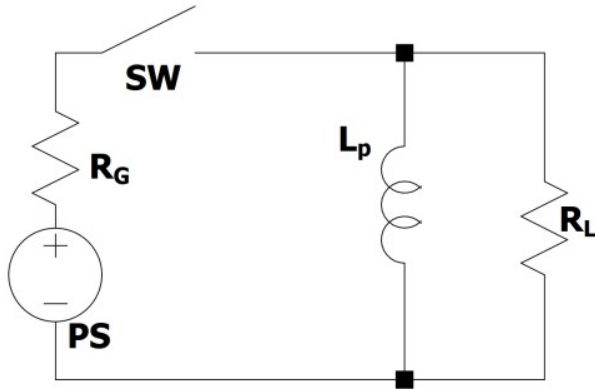


Fig. 8. Equivalent circuit for flat-top droop analysis.

$$D \approx \ln\left(\frac{1}{1-D}\right) = \frac{t R_L R_{PFN}}{L_P (R_L + R_{PFN})}. \quad (10)$$

The relationship between the primary inductance and the flat-top drop in the pulse transformer is shown as Fig. 9.

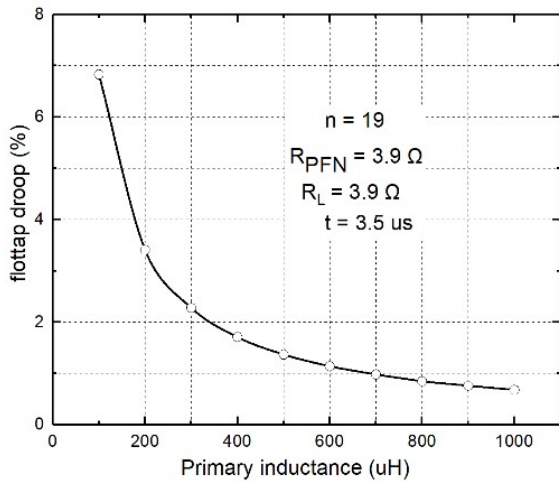


Fig. 9. The relationship between primary inductance and flat-top droop.

#### IV. RESULTS AND DISCUSSION

Figure 10 shows a picture of the high-voltage pulse transformer. The pulse transformer was installed inside a cylinder filled with electric insulating oil. A precise pulsed current sensor (0.1 V/A) installed in the secondary windings is used to convert pulse current to voltage for current measurement. A high-voltage divider (10850:1) close to the secondary side is used to measure the pulse voltage. Figure 11 shows output waveforms of pulse transformer. Table 3 summarizes the test param-

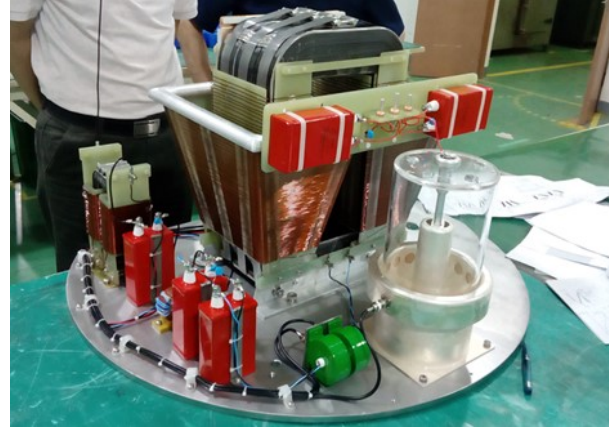


Fig. 10. Picture of the pulse transformer.

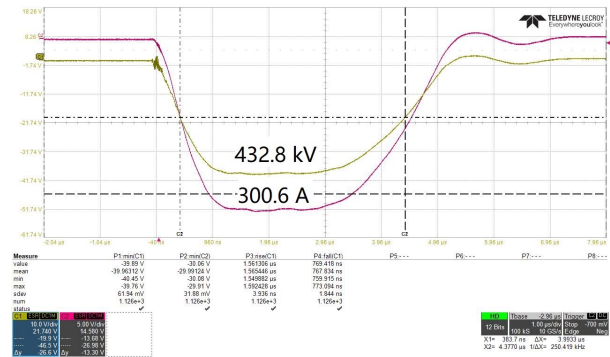


Fig. 11. Output waveform of the pulse transformer.

eters of the typical measured waveforms of the x-band high-power pulse transformer.

This paper presents the design process of the x-band klystron pulse transformer. Equivalent circuit modeling was used to analysis the leading edge and the fiat-top droop. It was indicated by relevant experimental data that the pulse transformer satisfied the requirements of the x-band 50 MW klystron.

Table 3: Test parameters of the waveform

Items	Value
Pulse voltage	432.8 kV
Pulse current	301 A
Leading edge	0.77 μs
Falling edge	1.56 μs
Flat-top	1.59 μs
FWHM	3.99 μs

## ACKNOWLEDGMENT

This project was supported by the National Natural Science Foundation of China (No.12005282) and Youth Innovation Promotion Association of Chinese Academy of Sciences (No. 2021283).

## REFERENCES

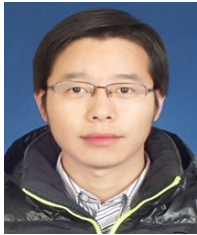
- [1] Z. Zhao, "The SXFEL upgrade: From test facility to user facility," *Applied Sciences*, vol. 12, Article no. 176, 2021.
- [2] A. Zavadtsev, D. Zavadtsev, O. Perevozchikova, and D. Churanov, "High-voltage pulse power supply system for klystron in transverse deflecting system of free-electron laser XFEL," *Journal of Physics: Conference Series*, vol. 1686, no. 1, Article no. 012070, 2020.
- [3] J. Tan, "Design, RF measurement, tuning, and high-power test of an X-band deflector for Soft X-ray Free Electron Lasers (SXFEL) at SINAP," *Nuclear Instruments and Methods in Physics Research Section A: Accelerators, Spectrometers, Detectors and Associated Equipment*, vol. 930, pp. 210-219, 2019.
- [4] A. Zavadtsev, "High-voltage pulse power supply system for klystron in transverse deflecting system of free-electron laser XFEL," *Journal of Physics: Conference Series*, vol. 1686, no. 1, Article no. 012070, 2020.
- [5] D. Aguglia, "Klystron modulator technology challenges for the Compact Linear Collider (CLIC)," *IEEE Pulsed Power Conference (PPC)*, Chicago, IL, USA pp. 1413-1421, 2011.
- [6] Y. F. Liu, "Analysis and optimization of high-power pulse transformer for SXFEL," *Nuclear Science and Techniques* vol. 30, no. 7, Article no. 109, 2019.
- [7] X. Deng, N. Liu, Y. Sun, Q. Guo, and M Zhang, "Design and analysis of a novel variable frequency transformer," *Applied Computational Electromagnetics Society (ACES) Journal*, vol. 33, no. 08, pp. 904-912, 2021.
- [8] D. Sprehn, "X-band klystron development at the Stanford Linear Accelerator Center," *Proceedings of SPIE 4031*, Orlando, FL, USA, 2000.
- [9] S. Candolfi, "Hybrid design optimization of high voltage pulse transformers for klystron modulators," *IEEE Transactions on Dielectrics and Electrical Insulation*, vol. 22, pp. 3617-3624, 2016.
- [10] X. Deng, K. Zheng, Y. Gu, A. Zhang, and Z. Jia, "Planar magnetic integration design based on LLC resonant converter," *Applied Computational Electromagnetics Society (ACES) Journal*, vol. 36, no. 11, pp. 1474-1483, 2021.
- [11] S. Blume, "Design and optimization procedure for high voltage pulse power transformers," *IEEE Transactions on Plasma Science*, vol. 43, pp. 3385-3391, 2015.
- [12] S. Kashyap, "Comparison of electromagnetic response in time and frequency domains," *Applied Computational Electromagnetics Society (ACES) Journal*, vol. 8, no. 2, pp. 17-43, 2022.
- [13] Y. Wang, "Optimal design and experimental study of pulse transformers with fast rise time and large pulse duration," *IEEE Transactions on Plasma Science*, vol. 42, pp. 300-306, 2014.
- [14] E. M. M. Costa, "Tesla transformer and its response with square wave and sinusoidal excitations," *Applied Computational Electromagnetics Society (ACES) Journal*, vol. 30, no. 9, pp. 1035-1040, 2021.
- [15] X. Liang, "An analytical method for pulse transformer-based inductive pulsed power supply circuit," *IEEE Transactions on Applied Superconductivity*, vol. 31, no. 8, Article no. 0500704, 2021.
- [16] T. Jalakas, "High-voltage pulse transformer for IOT modulators," *IET Electric Power Applications*, vol. 14, no. 12, pp. 2348-2354, 2020.
- [17] X. Chu, "A new solid-state LC-Marx generator based on saturable pulse transformer," *Review of Scientific Instruments*, vol. 92, no. 5, Article no. 054712, 2021.
- [18] F. Pan, "Design procedure of the leakage inductance for a pulse transformer considering winding structures," *IEEE Transactions on Plasma Science*, vol. 45, no. 9, pp. 2504-2510, 2017.
- [19] Y. F. Liu, H. Matsumoto, M. Gu, G. Q. Li and S. Li, "Design of an Oil-Immersed Pulse Modulator for X-Band 50-MW Klystron," *IEEE Transactions on Plasma Science*, vol. 51, no. 3, pp. 802-807, 2023.



**Yongfang Liu** received the Ph.D. degree from University of Chinese Academy of Sciences, Beijing, China in 2020. He is an electrical engineer with the Shanghai Synchrotron Radiation Facility, Shanghai Advanced Research Institute, Chinese Academy of Sciences, Shanghai. His research interests include pulsed power supply and pulsed magnet technologies, such as pulsed klystron modulators, linear transformer drivers, accelerator pulsed magnet and power supply.



**Yonghua Wu** was born in Anhui, China, in 1972. He is a member of the Shanghai Synchrotron Radiation Facility in Shanghai Advanced Research Institute, Chinese Academy of Sciences. His current research interests include high-voltage switch power supply, pulsed modulator power supply, such as line-type pulse modulators and solid-state pulsed modulators.



**Xiaoxuan Zhou** was born in Henan, China, in 1984. He received the M.S. degree in instrument Science and technology from the China Jiliang University, Hangzhou, in 2010. His current research interests include linear high-voltage pulse modulators, solid-state pulse modulators, pulsed magnet power supply and control techniques.



**Jin Tong** graduated from the University of Chinese Academy of Sciences, majoring in Nuclear Technology and Application. Since graduation, he has been engaged in the design of pulse magnets and magnetic measurement systems over years, especially for special magnets used in electron beam injection and extraction systems, such as linear/nonlinear kicker magnets, eddy current septum magnets and Lambertson cutting magnets, which have been designed and researched in large scientific facilities.